THE JOURNAL OF BIOLOGICAL CHEMISTRY VOL. 282, NO. 46, pp. 33530–33536, November 16, 2007

Dynamin Is Functionally Coupled to Insulin Granule Exocytosis*[S]

Received for publication, April 24, 2007, and in revised form, August 16, 2007 Published, JBC Papers in Press, September 11, 2007, DOI 10.1074/jbc.M703402200

Le Min[‡], Yuk M. Leung[§¶1], Alejandra Tomas[‖], Robert T. Watson[‡], Herbert Y. Gaisano[§], Philippe A. Halban[‖], Jeffrey E. Pessin[‡], and June Chunqiu Hou[‡2]

From the [‡]Department of Pharmacological Sciences, Stony Brook University, Stony Brook, New York 11794, the [§]Departments of Medicine and Physiology, University of Toronto, Toronto M5S 1A8, Canada, the [¶]Department of Physiology, China Medical University, Taichung 404, Taiwan, and the [‖]Department of Genetic Medicine and Development, Centre Médical Universitaire, 1 rue Michel-Servet, 1211 Geneva, Switzerland

The insulin granule integral membrane protein marker phogrin-green fluorescent protein was co-localized with insulin in Min6B1 β-cell secretory granules but did not undergo plasma membrane translocation following glucose stimulation. Surprisingly, although expression of a dominant-interfering dynamin mutant (Dyn/K44A) inhibited transferrin receptor endocytosis, it had no effect on phogrin-green fluorescent protein localization in the basal or secretagogue-stimulated state. By contrast, co-expression of Dyn/K44A with human growth hormone as an insulin secretory marker resulted in a marked inhibition of human growth hormone release by glucose, KCl, and a combination of multiple secretagogues. Moreover, serial pulse depolarization stimulated an increase in cell surface capacitance that was also blocked in cells expressing Dyn/K44A. Similarly, small interference RNA-mediated knockdown of dynamin resulted in marked inhibition of glucose-stimulated insulin secretion. Together, these data suggest the presence of a selective kiss and run mechanism of insulin release. Moreover, these data indicate a coupling between endocytosis and exocytosis in the regulation of β-cell insulin secretion.

In the basal state pancreatic β-cells secrete insulin at a low rate and following a meal increase insulin release into the circulation sufficient to maintain normal glucose homeostasis. Insulin is stored in β-cells as zinc hexamer crystals within mature granules that undergo tightly regulated exocytosis in response to extrinsic stimuli (such as glucose) that induce a cascade of events leading to the elevation of cytosolic calcium levels and/or of various second messengers (1–3). In turn, calcium functions to promote the fusion of pre-docked readily releasable granules similar to that of the calcium-regulated release of various other hormones and neurotransmitters in multiple neuroendocrine cell types (3).

In pancreatic β-cells, it is generally accepted that there are two populations of insulin secretory granules, the readily releasable pool that is responsible for the initial (first phase) insulin secretion and a second reserve pool that is responsible for a more prolonged (second phase) insulin secretion (4, 5). The readily releasable granule pool is apparently predocked at the cell surface with the Q-SNARE proteins, syntaxin 1 and SNAP25, in a complex with the granule R-SNARE protein VAMP2 and the calcium-regulated protein, synaptotagmin, although the specific synaptotagmin isoform remains unresolved (6–9). More recently, other studies have also indicated the involvement of the syntaxin 4 isoform in insulin secretion (10, 11). In any case, following the initial rapid first phase of insulin secretion, second phase secretion results from the recruitment of reserve granules to the plasma membrane that are also dependent on Q- and R-SNARE interaction for fusion.

Various models describing the mechanism of insulin granule fusion with the plasma membrane have been proposed. Initial studies have suggested that the release of the insulin-containing dense core granule content occurs *en masse*, consistent with the formation of a plasma membrane pore that fully expands to encompass the granule membrane proteins and lipids (12–14). Alternatively, it has also been suggested that insulin granules may actually stack and communicate with each other with a given granule releasing its content into another granule leading to a continuously gating channel to the plasma membrane through a process called compound exocytosis (15, 16). Another model has recently been proposed in that each granule separately forms a transient plasma membrane pore with the plasma membrane resulting in the release of intraluminal cargo, and either complete mixing of the membrane components (kiss and run) or selective membrane mixing (cavicapture) followed by endocytosis and recycling of the vesicle/granule membrane proteins and lipids (17–19). Although these studies examined the trafficking/release of single granule events, we have examined the macroscopic function of dynamin in the regulation of insulin secretion. Consistent with previous studies (18), inhibition of endocytosis does not lead to the appearance of the insulin granule membrane marker phogrin at the cell surface suggesting the transient opening of a selective granule-plasma membrane pore. Surprisingly however, expression of a dominant-interfering dynamin mutant or

* This work was supported in part by National Institutes of Health Grants DK33823 and DK55811, by the Swiss National Science Fund (Grants 3200B0-101902 and 310000-113967/1), and by the Canadian Institute of Health (Grant MOP-64465). The costs of publication of this article were defrayed in part by the payment of page charges. This article must therefore be hereby marked "*advertisement*" in accordance with 18 U.S.C. Section 1734 solely to indicate this fact.

[S] The on-line version of this article (available at http://www.jbc.org) contains supplemental data and Figs. S1–S3.

[1] Recipient of a post-doctoral fellowship from the Canadian Diabetes Association.

[2] To whom correspondence should be addressed: Dept. of Pharmacological Sciences, Stony Brook University, BST8-140, Stony Brook, NY 11794-8651. Tel.: 631-444-3059; Fax: 631-444-3022; E-mail: Hou@pharm.stonybrook.edu.

siRNA[3]-mediated dynamin knockdown resulted in a marked inhibition of insulin secretion. These data indicate the presence of a direct coupling between insulin granule exocytosis (fusion pore opening) and endocytosis (fusion pore closure) events.

EXPERIMENTAL PROCEDURES

Cell Culture and Transfection—Min6B1 (transformed mouse β) cells (20) were grown at 37 °C in 5% CO_2 in Dulbecco's modified Eagle's medium supplemented with 15% fetal bovine serum containing penicillin-streptomycin (100 units/ml and 100 μg/ml) and 71 μM 2-mercaptoethanol. INS-1E (transformed rat β) cells (21) were grown in RPMI 1640 media supplemented with 10% fetal bovine serum containing penicillin-streptomycin (100 units/ml and 100 μg/ml) as previously described (20, 21). For hGH secretory assays, the cells were transfected with 2 μg of hGH cDNA plus either 6 μg of empty vector (pCDNA 3.1) or the dominant-interfering dynamin mutant (Dyn/K44A) cDNA using Lipofectamine 2000 according to the manufacturer's instructions (Invitrogen). For confocal fluorescent microscopy examination, the cells were co-transfected with 2 μg of phogrin-GFP or transferrin receptor cDNAs with Dyk/K44A, respectively.

Dynamin 2 siRNA Knockdown and Immunoblotting—Min6B1 cells were grown on 15-cm dishes and electroporated with either 1 nmol of a scrambled or Dyn2-specific siRNA (Ambion) and cultured for 72 h. The cell lysates were subjected to SDS-PAGE and immunoblotted with a dynamin 2 antibody (Novus Biologicals), total dynamin antibody (Sigma), and a p115 antibody (BD Transduction Laboratory) as an internal control. Min6B1 cell lysate and mouse brain tissue extracts were blotted with dynamin 1 and dynamin 2 antibodies (Novus Biologicals) as control for tissue-specific dynamin expression.

hGH Secretion—The Min6B1 cells were plated in 60-mm (3×10^6 cells) coverslips for 24 h prior to transfection and were maintained for an additional 48 h post-transfection. The cells were then incubated in KRBH (4.7 mM KCl, 125 mM NaCl, 5 mM $NaHCO_3$, 1.2 mM $MgSO_4$, 1 mM $CaCl_2$, 25 mM HEPES, pH 7.4, 1.2 mM KH_2PO_4, and 0.1% bovine serum albumin) containing 2.8 mM glucose for 2 h and then mounted in a Zeiss perfusion closed POC-R system (20). After assembly of the perfusion chamber, the cells were perfused in KRBH containing 2.8 mM glucose for 15 min, and the perfusate was switched to KRBH buffer containing either 16.7 mM glucose, 30 mM KCl or a mixture of multiple secretagogues: BM (16.7 mM glucose, 10 nM forskolin, 1 mM isobutylmethylxanthine, and 30 mM KCl). The release of hGH into the medium was determined by an enzyme-linked immunosorbent assay (Roche Applied Science).

Insulin Secretion—The Min6B1 cells were transfected by electroporation with 1 nM of either the scrambled or Dyn2-specific siRNA for 72 h. The cells were then incubated in KRBH containing 2.8 mM glucose for 2 h and treated with 16.7 mM glucose for an additional 1 h. The release of insulin into the medium and total insulin content in the lysate were determined by an enzyme-linked immunosorbent assay (Mercodia).

Measurement of Membrane Capacitance—The whole cell configuration of the patch clamp technique was used to measure changes in cell membrane capacitance as previously described (22, 23). Briefly, electrodes were coated with orthodontic wax (Butler, Guelph, Ontario, Canada) close to the tips and heat-polished. Resistances ranged from 3.5 to 5 MΩ when pipettes were filled with the intracellular solution, which contained: 120 mM CsCl, 20 mM triethanolamine chloride, 1 mM $MgCl_2$, 0.1 mM EGTA, 10 mM HEPES, 0.1 mM cAMP, and 5 mM MgATP (pH 7.25 adjusted with CsOH). The extracellular solution contained: 140 mM NaCl, 4 mM KCl, 1 mM $MgCl_2$, 10 mM $CaCl_2$, 2 mM D-glucose, and 10 mM HEPES (pH 7.4 adjusted with NaOH). Cell capacitance was estimated by the Lindau-Neher technique, implementing the "Sine + DC" feature of the Lock-in module (40 mV peak-to-peak and a frequency of 500 Hz) in the standard whole cell configuration (22). Recordings were conducted using an EPC9 patch clamp amplifier and Pulse software. A train of six 500-ms depolarizing pulses (1-Hz stimulation frequency from −70 to 0 mV) elicited insulin granule exocytosis. The experimental temperature was set at 30 °C. In these experiments, the cells were transfected with GFP-Dyn/WT or GFP-Dyn/K44A to identify the specific cells for patch clamping.

Confocal Fluorescence—Min6B1 cells were plated in a 6-well plate with coverslips and transfected with phogrin-EGFP and Dyn/K44A. 48 h later, the cells were incubated in KRBH buffer containing 2.8 mM glucose for 2 h and then stimulated with either 16.7 mM glucose or BM for 1 h. Then the cells were fixed in 4% paraformaldehyde and incubated with various primary (insulin and dynamin antibodies from Sigma) and Texas Red-conjugated secondary antibodies (from Jackson ImmunoResearch Laboratory).

For live cell imaging experiments, Min6B1 cells were electroporated with phogrin-GFP in the presence or absence of Dyn2 siRNA (1 nmol). Cells were then plated on 35-mm glass bottom microwell dishes (Mat Tek corp.) or plated on a 35-mm coverslip for fixed images. Cells were imaged after a 72-h recovery period using a Zeiss LSM 510 scanning laser confocal microscope with 63×/1.4 numerical aperture Plan Apochromatic oil immersion objective lens and 488 nm laser excitation. A time series consisting of 200 images captured every 5 s was obtained for each cell. Stimulation was with BM as described above. Time series results were exported as QuickTime movies and text added using Adobe GoLive CS2. Movies were compressed using River Past Video Cleaner.

RESULTS

Integral Membrane Proteins in Insulin Granules Do Not Translocate to the Plasma Membrane—It is well established that, following fusion of transport vesicle compartments (donor membranes) with the plasma membrane (acceptor membrane), donor integral membrane cargo proteins are physically inserted into the acceptor membrane and are readily visualized at the cell surface by fluorescence microscopy. For example, the insulin stimulation of GLUT4 translocation in adipocytes or vasopressin stimulation of AQP2 translocation in collecting duct principal cells results in the visual redistribution of these proteins to the plasma membrane (24). We therefore

[3] The abbreviations used are: siRNA, small interference RNA; hGH, human growth hormone; Dyn, dynamin; EGFP, enhanced green fluorescent protein; WT, wild type.

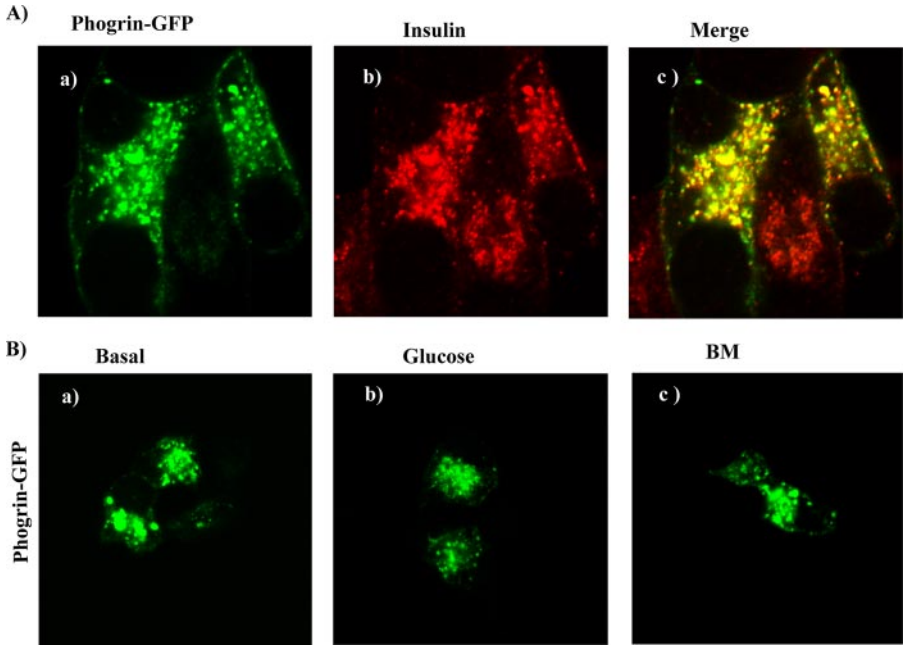

FIGURE 1. **Secretagogue stimulation does not result in a redistribution of phogrin from insulin granules to the plasma membrane.** *A*, Min6B1 cells were transfected with phogrin-GFP and 48 h later fixed and examined by confocal fluorescence microscopy for the co-localization of phogrin-GFP with endogenous insulin (*panels a–c*). *B*, Min6B1 cells were transfected with phogrin-GFP (*panels a–c*) and 48 h later either untreated (*Basal*, *panel a*) or stimulated with 16.7 mM glucose (*Glucose*, *panel b*) or the secretagogue mixture (*BM*, *panel c*). The cells were then fixed and examined by confocal fluorescence microscopy. These are representative images taken from three to four independent experiments.

expressed the integral insulin granule membrane protein phogrin as a GFP fusion construct, and, as previously reported (25), we observed a near identical co-localization with insulin containing intracellular compartments, presumably insulin granules (Fig. 1*A*, *panels a–c*). Although phogrin co-localized with these insulin granules, neither glucose nor the BM stimulatory mixture resulted in any detectable redistribution of phogrin to the cell surface membrane (Fig. 1*B*, *panels a–c*). These data indicate that the insulin granule membrane protein phogrin did not undergo full fusion with the plasma membrane during insulin granule exocytosis.

To confirm this observation, we also performed live cell imaging of Min6B1 cells expressing phogrin-GFP (supplementary Fig. 1S). These images demonstrate that phogrin-GFP-containing granules are in dynamic motion but that secretagogue stimulation does not appreciably change the rate of intracellular trafficking or the accumulation of phogrin at the cell surface. Together, these data are consistent with recent reports indicating that the release of insulin occurs by a kiss and run or cavicapture type mechanism, which limits the mixing of insulin granule membrane contents with the plasma membrane (17).

All membrane proteins are thought to undergo continuous cycling from one compartment to another, albeit at different rates. Therefore, if phogrin does translocate to the plasma membrane, inhibition of endocytosis should result in an accumulation of phogrin at the cell surface. To further assess such possible phogrin translocation to the plasma membrane, we therefore examined the effect of blocking plasma membrane endocytosis on the cell surface accumulation of phogrin (Fig. 2). In the basal state, co-expression of the dominant-interfering dynamin mutant (Dyn/K44A) had no significant effect on the distribution of phogrin (Fig. 2*A*, *panels a–c*). Even more surprisingly, glucose stimulation in the presence of Dyn/K44A also did not result in any significant redistribution of phogrin (Fig. 2*A*, *panels d–f*). To ensure that Dyn/K44A inhibited plasma membrane endocytosis, the cells were co-transfected with transferrin receptor plus either empty vector or Dyn/K44A. Under these conditions, labeling of the transferrin receptor at the cell surface at 4 °C following by warming the cells to 37 °C for 30 min resulted in the expected internalization of the transferrin receptor (Fig. 2*B*, *panels a* and *e*). However, in the presence of Dyn/K44A the internalization of the transferrin receptor was efficiently inhibited (Fig. 2*B*, *panels b–d* and *f–h*). These data demonstrate that, although inhibition of endocytosis by Dyn/K44A results in the accumulation of general trafficking membrane proteins such as transferrin receptor at the cell surface, there was no effect on the cell surface localization of the insulin granule marker phogrin.

Inhibition of Plasma Membrane Endocytosis Blocks Secretagogue-stimulated Insulin Secretion—As described above, because phogrin did not accumulate at the plasma membrane even when endocytosis was inhibited, we next examined the effect of Dyn/K44A on insulin secretion (Fig. 3). Min6B1 cells were co-transfected with either the empty vector or Dyn/K44A plus a plasmid encoding hGH, because previous studies have established that hGH functions as a marker of insulin secretion (26, 27) thus allowing for secretion only from (co-)transfected cells to be monitored. Expression of Dyn/K44A had no significant effect on basal release of hGH compared with control cells (Fig. 3*A*). Glucose stimulation of control cells resulted in an approximate 6-fold increase in hGH release. By contrast, expression of Dyn/K44A markedly blunted the extent of glucose-stimulated hGH release that resulted in only an approximate 2.5-fold increase in secretion. This occurred without any significant change in the total amount of growth hormone content (Fig. 3*B*).

The inhibition of glucose-stimulated hGH release in the media could have resulted from a reduction in either first phase secretion and/or second phase secretion. To assess the effect of Dyn/K44A on the dynamics of insulin secretion, we next examined the time-course of hGH secretion in transfected Min6B1 cells that were subjected to perifusion (Fig. 4). In control cells, glucose stimulation resulted in a rapid rise in the rate of hGH release that was maximal at ~5 min and then began to decline (Fig. 4*A*). Although these cells do not display a robust glucose-stimulated second phase secretion, a small shoulder was appar-

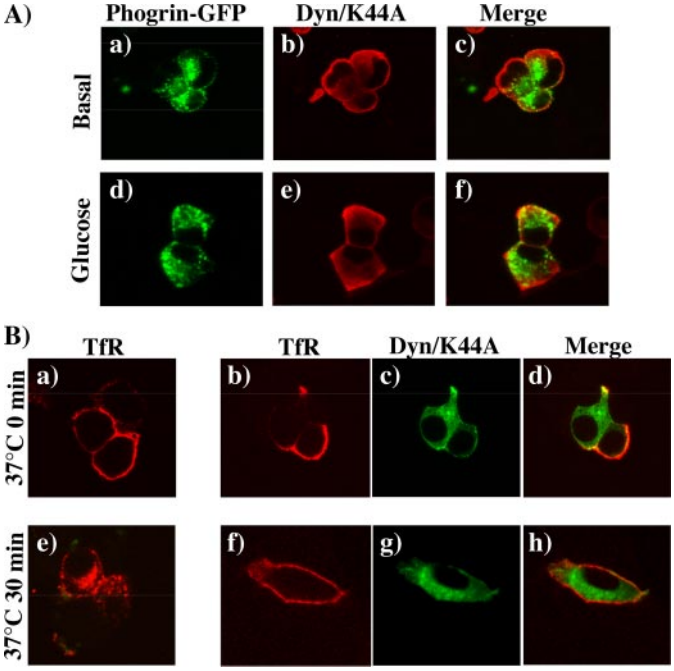

FIGURE 2. **Expression of dominant-interfering dynamin mutant (Dyn/K44A) does not result in the accumulation of phogrin at the plasma membrane.** *A*, Min6B1 cells were co-transfected with phogrin-GFP and Dyn/K44A and 48 h later the cells were either left untreated (*panels a–c*) or stimulated with 16.7 mM glucose (*panels d–f*). The cells were fixed and subjected to confocal fluorescent microscopy for phogrin-GFP (*panels a* and *d*), Dyn/K44A (*panels b* and *e*). *Merged images* are shown in *panels c* and *f*. These are representative images taken from three independent experiments. *B*, Min6B1 cells were co-transfected with the transferrin receptor cDNA and empty vector (*panels a* and *e*). 48 h later the cells were cooled to 4 °C, and the surface-exposed transferrin receptor was labeled with Texas Red-conjugated transferrin. The cells were then either fixed right after 4 °C labeling (time 0) or warmed to 37 °C for 30 min following by fixation and subjected to confocal fluorescent microscopy (*panels a* and *e*). In parallel, the Min6B1 cells were co-transfected with the transferring receptor and dominant-interfering dynamin mutant (Dyn/K44A), and cells were labeled with Texas Red-transferrin at 4 °C. The cells either fixed right after 4 °C labeling (time 0) or warmed to 37 °C for 30 min following by fixation and subjected to confocal fluorescent microscopy for transferring (*panels b* and *f*), Dyn/K44A (*panels c* and *g*). *Merged images* are shown in *panels d* and *h*. These are representative images taken from three independent experiments.

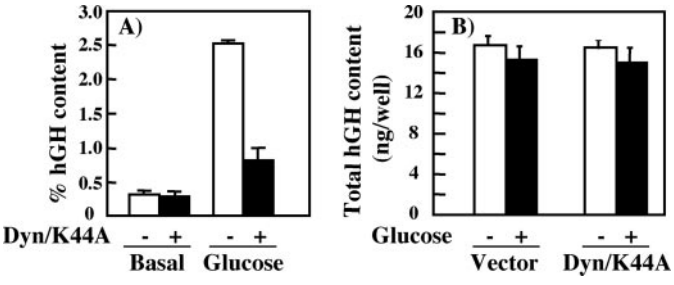

FIGURE 3. **Expression of Dyn/K44A inhibits glucose-stimulated insulin secretion.** *A*, Min6B1 cells were co-transfected the hGH cDNA with either the empty vector or Dyn/K44A. 48 h later the cells were either left untreated (*open boxes*) or incubated with 16.7 mM glucose (*solid boxes*) for 60 min. The media were collected and assayed for the presence of hGH. *B*, the total hGH content was determined from the transfected cells in *A* by preparation of total cell extracts and assayed for the presence of hGH. These data are the average from three independent experiments.

ent that probably represents second phase secretion. Consistent with the total secretion data, expression of Dyn/K44A markedly reduced both the initial and the extended time course of insulin secretion.

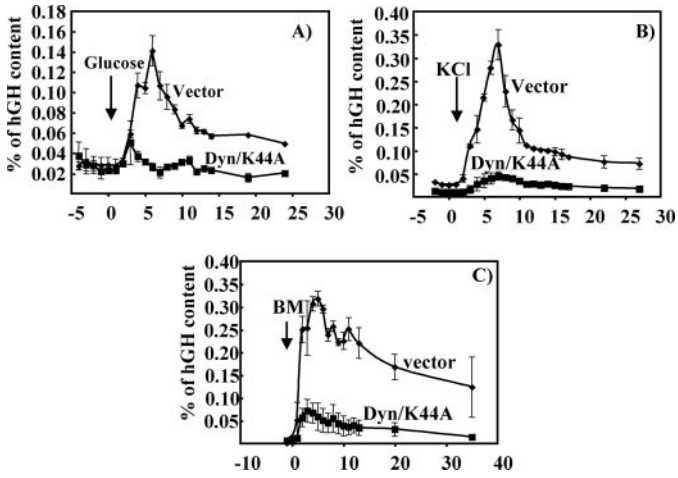

FIGURE 4. **Expression of Dyn/K44A inhibits glucose, KCl, and secretagogue mixture (BM)-stimulated insulin secretion time course.** Min6B1 cells were co-transfected the hGH cDNA and either the empty vector or Dyn/K44A. 48 h later the cells were placed in a perifusion chamber and at the time indicated the cells were perifused with either 16.7 mM glucose (*A*), 30 mM KCl (*B*), or the BM secretagogue mixture (*C*). The perifusate was collected at the times indicated and assayed for the release of hGH. These are representative experiment independently performed three to four times.

To determine whether this was specific to glucose or a general phenomenon for multiple secretagogues, we next examined the effect of KCl-mediated cellular depolarization (Fig. 4*B*). In control cells, KCl induced a robust first phase release of hGH that was also maximal by ~7 min and then declined toward basal secretory levels by 25 min. As observed for glucose stimulation, cells expressing Dyn/K44A displayed a marked reduction in the extent and rate of KCl-induced hGH release. Because depolarization-induced insulin secretion only stimulates first phase release (28), these data indicate that expression of Dyn/K44A inhibits first and second phase insulin secretion.

We also determined whether the expression of Dyn/K44A could inhibit insulin secretion when stimulated by a strong mixture of multiple secretagogues. The BM secretagogue mixture (glucose, isobutylmethylxanthine, and KCl) is a very potent simulator of both first and second phase insulin secretion in Min6B1 cells (29). As expected, the combination of secretagogues in the BM mixture induced a striking increase in the rate of insulin secretion with an approximate 15-fold stimulation (Fig. 4*C*). Similar to the effect on glucose- and KCl-stimulated hGH secretion, expression of Dyn/K44A inhibited both initial and extended phases of hGH secretion. A comparison of the area under the curve values indicated that Dyn/K44A inhibited glucose, KCl, and the BM secretagogue mixture to similar extents (72.4 ± 4.7%, 77.6 ± 3.1%, and 78.4 ± 13% inhibition, respectively). Together, these data demonstrate that in the presence of Dyn/K44A there is a marked inhibition of secretagogue-stimulated granule content exocytosis.

Dynamin Function Is Required for Granule Fusion with the Plasma Membrane—If dynamin function was necessary for the release of granule content, then we would predict that at a macroscopic level the fusion/opening of granules in the presence of Dyn/K44A would be reduced thereby preventing insertion of additional membrane content to the plasma membrane. To test this hypothesis, we determined the changes in total plasma membrane capacitance following a train of depolarizing voltage

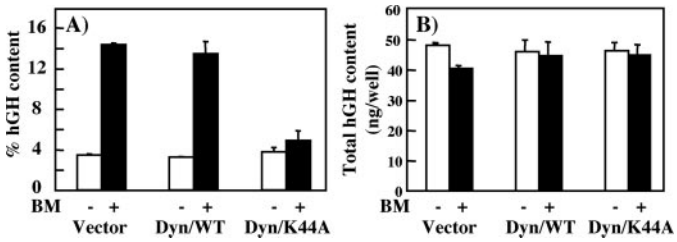

FIGURE 5. **Expression of Dyn/K44A in INS1 cells inhibits secretagogue mixture (BM)-stimulated insulin secretion.** *A*, INS1 cells were co-transfected the hGH cDNA with either the empty vector, Dyn/WT, or Dyn/K44A. 48 h later the cells were left untreated (*open boxes*) or stimulated with the BM secretagogue mixture (*solid boxes*) for 60 min. The media were collected and assayed for the presence of hGH. *B*, the total hGH content was determined from the transfected cells in *A* by preparation of total cell extracts and assayed for the presence of hGH. These data are the average from two independent experiments.

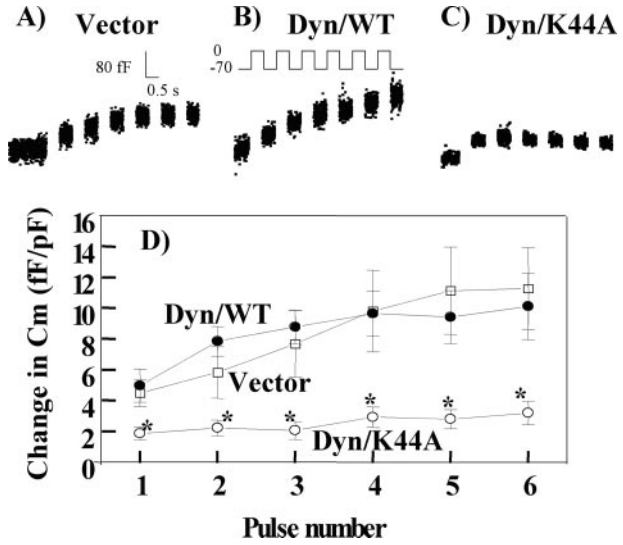

FIGURE 6. **Dyn/K44A inhibits pulse-depolarization induced changes in membrane capacitance.** INS1 cells were either untransfected (*A*), transfected with a GFP-Dyn/WT (*B*), or with GFP-Dyn/K44A (*C*). Membrane capacitance (C_m) was triggered by a train of six 500-ms depolarizing pulses, 1-Hz stimulation frequency) from −70 to 0 mV. *D*, the changes in C_m were normalized to cell size and plotted against the pulse number. All values are mean ± S.E. of 7–11 cells. *, $p <$ 0.05 compared with Dyn/WT control and untransfected cells.

by patch clamp recordings. However, because Min6B1 cells were difficult to patch clamp, we first determined whether Dyn/K44A would inhibit secretagogue-stimulated secretion from the INS-1E β-cell line that is more amenable to patch clamping (Fig. 5). Although this cell line does not display a robust glucose-stimulated insulin secretion, it is highly responsive to the BM secretagogue mixture. As observed for the Min6B1 cells, BM stimulation resulted in a marked increase in hGH secretion in the empty vector and Dyn/WT co-transfected cells, whereas there was a dramatic inhibition of hGH secretion in the INS-1E cells transfected with Dyn/K44A (Fig. 5*A*). Similar to the Min6B1 cells, the Dyn/K44A-dependent inhibition of secretion occurred without any significant change in the total hGH reporter content (Fig. 5*B*).

Having observed the similar phenomenon in INS-1E cells, we next examined the changes in total plasma membrane capacitance following a train of depolarizing voltage by patch clamp recordings (Fig. 6). As expected, serial depolarization triggered membrane capacitance (C_m) increases (exocytosis) in untransfected cells that tended to saturate following multiple depolarizing pulses (Fig. 6*A*). To determine the effect of dynamin expression, we transfected INS1-1E cells with Dyn/WT and Dyn/K44A containing a GFP tag to identified the transfected cell populations. Expression of Dyn/WT also resulted in increased membrane capacitance following depolarizing pulses essentially identical to that observed for the non-transfected INS-1E cells (Fig. 6*B*). However, in marked contrast, there was a near complete inhibition of the depolarization induction of membrane capacitance increase (Fig. 6*C*). Quantitative results are summarized in Fig. 6*D* and demonstrate that Dyn/K44A results in a major impairment in depolarization-stimulated increase in membrane capacitance consistent with a defect in insulin granule exocytotic fusion.

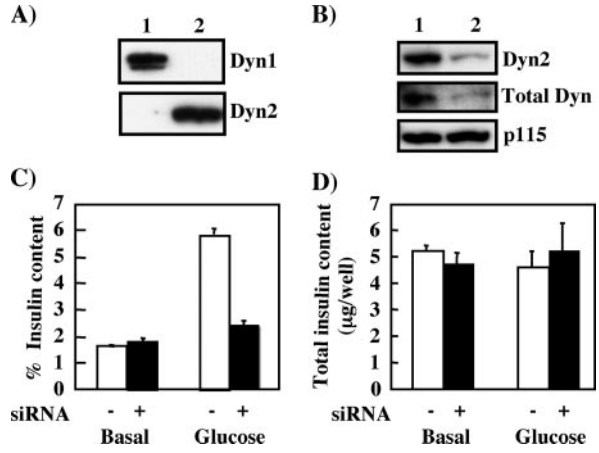

FIGURE 7. **siRNA-mediate dynamin 2 knockdown inhibits glucose-stimulated insulin secretion.** *A*, mouse brain tissue extract (*lane 1*, 25 μg) and Min6B1 cell lysate (*lane 2*, 25 μg) were immunoblotted with a dynamin 1 (*Dyn1*)- or a dynamin 2 (*Dyn2*)-specific antibody. *B*, Min6B1 cells were transfected with 1 nM either the scrambled (*lane 1*) or dynamin 2-specific siRNA (*lane 2*). 72 h later the cell extracts were prepared, and 25 μg of protein was immunoblotted using the dynamin 2 antibody, a total (pan) dynamin antibody or the p115 antibody as described under "Experimental Procedures." *C*, Min6B1 cells were transfected with 1 nM either the scrambled or dynamin 2-specific siRNA. 72 h later the cells were either left untreated (*open boxes*) or incubated with 16.7 mM glucose (*solid boxes*) for 60 min. The media were collected and assayed for the presence of released insulin. *D*, the total insulin content was determined by preparation of total cell extracts. These data are the average from three independent experiments.

siRNA-mediated Dynamin Knockdown Inhibits Glucose-stimulated Insulin Secretion—Because the above data were obtained from co-transfection of a dominant-interfering dynamin mutant and with hGH as an insulin secretion marker, we subsequently examined the effect of siRNA-mediated reduction of dynamin on endogenous insulin secretion. It is well known that dynamin 1 is primarily expressed in neural tissues, whereas dynamin 2 is ubiquitously expressed and dynamin 3 expression is restricted to the testes with low levels in the lung and nervous tissue (30). Because insulin-secreting β-cells are neuroendocrine-like, we then examined the relative expression of the dynamin isoforms in the Min6B1 cells. As shown in Fig. 7*A* (*upper panel*), dynamin 1 was readily detected in mouse brain extracts (*lane 1*) with essentially no detectable expression in Min6B1 cells (*lane 2*). By contrast, immunoblotting with the dynamin 2 antibody (*lower panel*) demonstrated the presence of dynamin 2 in Min6B1 cell (*lane 2*) with very low levels in the mouse brain extract (*lane 1*). Because dynamin 2

was relatively more abundant in the Min6B1 cells, the cells were then transfected with either a scrambled siRNA or a dynamin 2-specific siRNA (Fig. 7*B*). 72 h following transfection there was an approximate 90% reduction of dynamin 2 protein levels compared with the scrambled siRNA-transfected cells (*upper panel*, *lanes 1* and *2*). The reduction of dynamin 2 protein was specific, as p115 protein levels remained unchanged (*lower panel*). Moreover, immunoblotting with a total (pan) dynamin antibody that detects all three dynamin isoforms demonstrated an identical extent of dynamin protein reduction compared with the dynamin 2-specific antibody (*middle panel*). These data demonstrated that dynamin 2 is the predominant isoform in Min6B1 cells and that the dynamin 2-specific siRNA was highly effective in reducing dynamin protein levels.

Having demonstrated the effectiveness of the dynamin 2 siRNA, we assessed the effect of dynamin protein reduction on glucose-stimulated insulin secretion. The dynamin 2 knockdown had no significant effect on basal release of endogenous insulin compared with control cells (Fig. 7*C*). In scrambled siRNA-transfected cells, glucose stimulation resulted in an approximate 3.5-fold increase in insulin release. By contrast, the knockdown of dynamin 2 markedly reduced the extent of glucose-stimulated insulin release and resulted in only an approximate 1.2-fold increase of insulin secretion. This occurred without any significant change in the total amount of insulin content (Fig. 7*D*). Similar to the expression of Dyn/K44A, we also did not detect any significant redistribution of phogrin-GFP in the Dynamin siRNA knockdown cells either in fixed images or by live cell imaging (supplemental Figs. 2S and 3S). Together, these data strongly support a required role for dynamin function in regulating the extent of insulin secretion (insulin granule exocytosis).

DISCUSSION

Various studies have suggested that insulin granules undergo complete fusion resulting in the total mixing of granule membrane proteins and lipids with the plasma membrane (12–14). Alternatively, other studies have suggested that the insulin granules transiently open a fusion pore to allow intraluminal contents to diffuse out followed by membrane closure. This latter process can either be non-selective (kiss and run) or selective (cavicapture) such that granule membrane proteins/lipids either mix or remain segregated from the bulk plasma membrane, respectively (17–20).

More recently, confocal fluorescence and total internal reflection fluorescence microscopy of soluble insulin granule tracers detected the presence of plasma membrane compartments that appeared to undergo full fusion (6, 13, 14, 31, 32). By contrast, total internal reflection fluorescence microscopy examination of insulin granule membrane proteins indicated that, although small molecular weight proteins (VAMP2 and synaptotagmin I) were incorporated into the plasma membrane, the large granule membrane protein phogrin was found excluded from the plasma membrane and remained granule-associated (17). Moreover, the larger soluble insulin granule marker, tissue plasminogen activator-monomeric red fluorescent protein, was retained much longer than the small soluble marker, neuropeptide Y-monomeric red fluorescent protein. It was therefore concluded that insulin release resulted from the transient opening of a selective fusion pore (17, 19, 33).

Consistent with these latter studies, we have also observed that the extent of phogrin incorporation into the plasma membrane following glucose stimulation is below visual detection by fluorescence microscopy. However, in contrast to phogrin in insulin-secreting cells, most other membrane proteins undergo continuous plasma membrane recycling, albeit at different rates, independent of their steady-state intracellular localization. For example, furin and TGN38 are predominantly localized to the trans-Golgi network but transiently traffic to and from the plasma membrane (34–36). This is readily detected by the inhibition of plasma membrane endocytosis that results in their slow accumulation at the plasma membrane. Thus, we reasoned that if phogrin slowly cycled to the plasma membrane it would become apparent if endocytosis was blocked by the expression of the dominant-interfering dynamin mutant. However, inhibition of plasma membrane endocytosis, as assessed by transferrin receptor recycling, did not result in any appreciable cell surface accumulation of phogrin in either the basal or stimulated-state. These results indicate that insulin granules did not undergo full fusion with the plasma membrane, and they are consistent with a selective cavicapture type of fusion pore opening with only a limited extent of granule membrane mixing with the plasma membrane.

More surprisingly, expression of Dyn/K44A or the siRNA-mediated dynamin 2 knockdown markedly reduced the extent of insulin secretion stimulated by glucose, KCl, and a combination of multiple secretagogues. Furthermore, examination of the time course of insulin release demonstrated that both first and second phase insulin secretion was inhibited. In agreement with these effects on insulin secretion, the depolarization-induced increase in membrane capacitance was also markedly blunted in the presence of Dyn/K44A. Although our data were unable to clearly distinguish between first and second phase insulin secretion, the effect of blocking dynamin function on secretory granule release has previously been observed in chromaffin cells by using catecholamine amperometry combined with different patterns of stimulation (37). These results demonstrated that anti-dynamin IgG antibody progressively reduced the total amount of catecholamine release following successive rounds of stimulation, suggesting a primary effect on second phase secretion.

In any case, because dynamin is well established to function in the endocytotic process, one possibility is that the extent of granule exocytosis is directly coupled to endocytosis in a manner necessary to prevent unrestricted expansion of the plasma membrane surface area. Although this is an appealing hypothesis, dynamin has recently been observed to undergo trafficking to the sites of insulin release, whereas other recognized endocytotic proteins such as clathrin, epsin, and amphiphysin are not selectively recruited (17). Moreover, because insulin granules are relatively large (300 nm), it is unlikely that granule fission occurs via a clathrin-mediated process. Because under these conditions dynamin is unlikely to function in classic endocytosis, another mechanism must account for its requirement in the continuation of insulin release. In this regard, an alternative secretory model has been proposed in which insulin

granules are stacked together into a three-dimensional array beneath the plasma membrane, termed sequential exocytosis (15, 38, 39). As the plasma membrane bound granules open and close the fusion pore, the attached granules generate additional fusion pores that open and close connecting one granule to the next and thereby forming a chain leading to the plasma membrane. In this granule-granule fusion model, dynamin would therefore not function in classic endocytosis but would regulate the closing of fusion pores between granules.

This compound exocytosis model is also appealing, because it would account for the apparent inconsistency between a stable increase in membrane capacitance (increased plasma membrane mass) and the kiss and run/cavicapture model. In the kiss and run model, during the initial cargo release phase bulk membrane capacitance would be expected to increase; however, following closure of the transient fusion pore, membrane capacitance would decrease and return to the basal state in parallel to the changes in first and second phase insulin secretion. However, the changes in membrane capacitance remained relatively stable through each depolarization step, suggesting a continuous addition of membrane mass consistent with a complete fusion and membrane-mixing model. The compound exocytosis model can account for both results, because for a single granule the fusion pore can open and close transiently, but at the macroscopic level the multiple openings and closing would result in a steady-state (averaged) increase in membrane surface area. Moreover, this would also account for the relative ability of a small amount of granule SNARE proteins (VAMP2/synaptotagmin) to become incorporated into the plasma membrane but the bulk majority of the granule protein resident proteins (phogrin) to be excluded.

Finally, it is important to recognize that total internal reflection fluorescence microscopy of single granule fusion events was reported to be unaffected by the expression of a dominant-interfering dynamin mutant (40). In contrast to this, our data demonstrate a marked reduction in the extent of insulin secretion. These observations are similar to those observed for chromaffin granule release in Munc18a knock-out mice (41). In this system, single granule release events have identical kinetic and biophysical properties in the control and knock-out mice; however, the number of granule release events is markedly reduced in the absence of Munc18a. These differences in microscopic *versus* macroscopic events may underlie the specific mechanisms involved in insulin secretion. The simplest explanation is the presence of limited fusion sites, such that dynamin-dependent granule fission is required for the empty insulin granule to be released from the fusion site allowing for the docking of a new cargo-loaded insulin granule.

Acknowledgment—We thank Dr. Li Xie for technical support.

REFERENCES

1. Berggren, P. O., and Larsson, O. (1994) *Biochem. Soc. Trans.* **22,** 12–18
2. Mears, D. (2004) *J. Membr. Biol.* **200,** 57–66
3. Barg, S. (2003) *Pharmacol. Toxicol.* **92,** 3–13
4. Barg, S., Eliasson, L., Renstrom, E., and Rorsman, P. (2002) *Diabetes* **51,** Suppl. 1, S74–S82
5. Rorsman, P., Eliasson, L., Renstrom, E., Gromada, J., Barg, S., and Gopel, S. (2000) *News Physiol. Sci.* **15,** 72–77
6. Ohara-Imaizumi, M., Nishiwaki, C., Nakamichi, Y., Kikuta, T., Nagai, S., and Nagamatsu, S. (2004) *Diabetologia* **47,** 2200–2207
7. Nevins, A. K., and Thurmond, D. C. (2005) *J. Biol. Chem.* **280,** 1944–1952
8. Mizuta, M., Kurose, T., Miki, T., Shoji-Kasai, Y., Takahashi, M., Seino, S., and Matsukura, S. (1997) *Diabetes* **46,** 2002–2006
9. Brown, H., Meister, B., Deeney, J., Corkey, B. E., Yang, S. N., Larsson, O., Rhodes, C. J., Seino, S., Berggren, P. O., and Fried, G. (2000) *Diabetes* **49,** 383–391
10. Saito, T., Okada, S., Yamada, E., Ohshima, K., Shimizu, K., Shimomura, K., Sato, M., Pessin, J. E., and Mori, M. (2003) *J. Biol. Chem.* **278,** 36718–36725
11. Spurlin, B. A., and Thurmond, D. C. (2006) *Mol. Endocrinol.* **20,** 183–193
12. Orci, L., Amherdt, M., Malaisse-Lagae, F., Rouiller, C., and Renold, A. E. (1973) *Science* **179,** 82–84
13. Takahashi, N., Kishimoto, T., Nemoto, T., Kadowaki, T., and Kasai, H. (2002) *Science* **297,** 1349–1352
14. Ma, L., Bindokas, V. P., Kuznetsov, A., Rhodes, C., Hays, L., Edwardson, J. M., Ueda, K., Steiner, D. F., and Philipson, L. H. (2004) *Proc. Natl. Acad. Sci. U. S. A.* **101,** 9266–9271
15. Leung, Y. M., Sheu, L., Kwan, E., Wang, G., Tsushima, R., and Gaisano, H. (2002) *Biochem. Biophys. Res. Commun.* **292,** 980–986
16. Kwan, E. P., and Gaisano, H. Y. (2005) *Diabetes* **54,** 2734–2743
17. Tsuboi, T., McMahon, H. T., and Rutter, G. A. (2004) *J. Biol. Chem.* **279,** 47115–47124
18. Tsuboi, T., Zhao, C., Terakawa, S., and Rutter, G. A. (2000) *Curr. Biol.* **10,** 1307–1310
19. Taraska, J. W., Perrais, D., Ohara-Imaizumi, M., Nagamatsu, S., and Almers, W. (2003) *Proc. Natl. Acad. Sci. U. S. A.* **100,** 2070–2075
20. Lilla, V., Webb, G., Rickenbach, K., Maturana, A., Steiner, D. F., Halban, P. A., and Irminger, J. C. (2003) *Endocrinology* **144,** 1368–1379
21. Asfari, M., Janjic, D., Meda, P., Li, G., Halban, P. A., and Wollheim, C. B. (1992) *Endocrinology* **130,** 167–178
22. Lindau, M., and Neher, E. (1988) *Pflügers Arch.* **411,** 137–146
23. Lam, P. P., Leung, Y. M., Sheu, L., Ellis, J., Tsushima, R. G., Osborne, L. R., and Gaisano, H. Y. (2005) *Diabetes* **54,** 2744–2754
24. Procino, G., Caces, D. B., Valenti, G., and Pessin, J. E. (2005) *Am. J. Physiol.* **290,** F985–F994
25. Ohara-Imaizumi, M., Nakamichi, Y., Tanaka, T., Katsuta, H., Ishida, H., and Nagamatsu, S. (2002) *Biochem. J.* **363,** 73–80
26. Cheviet, S., Coppola, T., Haynes, L. P., Burgoyne, R. D., and Regazzi, R. (2004) *Mol. Endocrinol.* **18,** 117–126
27. Iezzi, M., Regazzi, R., and Wollheim, C. B. (2000) *FEBS Lett.* **474,** 66–70
28. Daniel, S., Noda, M., Straub, S. G., and Sharp, G. W. (1999) *Diabetes* **48,** 1686–1690
29. Donelan, M. J., Morfini, G., Julyan, R., Sommers, S., Hays, L., Kajio, H., Briaud, I., Easom, R. A., Molkentin, J. D., Brady, S. T., and Rhodes, C. J. (2002) *J. Biol. Chem.* **277,** 24232–24242
30. Urrutia, R., Henley, J. R., Cook, T., and McNiven, M. A. (1997) *Proc. Natl. Acad. Sci. U. S. A.* **94,** 377–384
31. Lindau, M., and Almers, W. (1995) *Curr. Opin. Cell Biol.* **7,** 509–517
32. Zenisek, D., Steyer, J. A., Feldman, M. E., and Almers, W. (2002) *Neuron* **35,** 1085–1097
33. Nagai, T., Ibata, K., Park, E. S., Kubota, M., Mikoshiba, K., and Miyawaki, A. (2002) *Nat. Biotechnol.* **20,** 87–90
34. Mallet, W. G., and Maxfield, F. R. (1999) *J. Cell Biol.* **146,** 345–359
35. Takahashi, S., Nakagawa, T., Banno, T., Watanabe, T., Murakami, K., and Nakayama, K. (1995) *J. Biol. Chem.* **270,** 28397–28401
36. Reaves, B., Horn, M., and Banting, G. (1993) *Mol. Biol. Cell* **4,** 93–105
37. Elhamdani, A., Palfrey, H. C., and Artalejo, C. R. (2001) *Neuron* **31,** 819–830
38. Orci, L., and Malaisse, W. (1980) *Diabetes* **29,** 943–944
39. Bokvist, K., Holmqvist, M., Gromada, J., and Rorsman, P. (2000) *Pflügers Arch.* **439,** 634–645
40. Tsuboi, T., Terakawa, S., Scalettar, B. A., Fantus, C., Roder, J., and Jeromin, A. (2002) *J. Biol. Chem.* **277,** 15957–15961
41. Voets, T., Toonen, R. F., Brian, E. C., de Wit, H., Moser, T., Rettig, J., Sudhof, T. C., Neher, E., and Verhage, M. (2001) *Neuron* **31,** 581–591